CVGIP: Graphical Models and Image Processing, Academic Press, 60(5), pp. 331-348, September 1998.

Contour-Based Warping

Kwai Hung Chan Rynson W.H. Lau

Computer Graphics and Media Laboratory

Department of Computing

The Hong Kong Polytechnic University, Hong Kong

Paper Title : *Contour-Based Warping*

Contact Author : *Dr. Rynson W.H. Lau*

Address : *Department of Computer Science*

City University of Hong Kong

Tat Chee Avenue, Kowloon, Hong Kong

Telephone No. : *(852) 2788-7525*

Fax No. : *(852) 2788-8614*

Email : *rynson@cs.cityu.edu.hk*

Contour-Based Warping

Abstract

In this paper, a new warping technique called contour-based warping is presented. Feature contours of objects are defined and mapped to their target shapes. This allows the user greater flexibility in defining the warping with minimal effort. Two image warping methods are introduced in this paper and both are based on the concept of mapping contours. The *peel-and-resample* method can warp simple image objects with a single inner-feature in a short time, but suffers from the problems of misalignment and inability of handling multiple features. The *wave propagation* method solves these two problems. Unlike most existing methods, this method warps image objects based on specified feature contours instead of points or vectors. Results of this method demonstrate that increasing the number of contour features distributed on the warping image reduces the computational time. However, it is slower compared with the peel-and-resample method when warping simple image objects with a single inner-feature.

1 Introduction

Image warping is the geometrical mapping of an image from one spatial domain (the source shape) onto another (the target shape). Digital image warping involves issues such as spatial transformation, resampling and antialiasing. This has been extensively discussed in [10][19]. Various image warping techniques were proposed and different results were obtained. They can be categorized into three main types of methods - *patch-based*, *point-based* and *vector-based* warping methods.

In patch-based warping, the spatial domain of the source image is firstly subdivided into a set of small patches. Then another set of patches is obtained by similar subdivision of the target image. The image is warped by transforming each patch of the source to its corresponding patch of the target. The pioneer of this type of method is the 2-pass mesh warping algorithm [17]. With this technique, a 2-pass transformation replaces a 2-D transformation with a sequence of orthogonal 1-D transformations. There are also investigations of other patch-based warping methods such as [8][11] which map triangular patch-pairs.

In point-based warping, important points are used as the basic corresponding mapping feature pairs. Many point-based methods treat warping as a scattered-data interpolation function. Specific interpolation functions which can interpolate through all feature points are used. A warping technique based on radial basis function was introduced in [1] and was applied in synthesizing simple facial expression. Radial basis function is an effective function in multivariate interpolation of scattered data without preferred orientation. A similar approach was presented in [2][4]. Instead of radial basis function, they use thin plate splines as the basis of the interpolation function. Another point-based method [12][13] handles the warping as a free-form deformation problem depending on 2D feature points. A more complete discussion of point-based warping is given in [14].

Vector-based warping techniques use vector pairs as the basis of the warping transformation. Vector-based image warping was firstly proposed by Beier and Neely [3]. A vector pair defines a coordinate mapping between them. The displacement of any point in the image is then a weighted sum of the mappings due to all specified vector feature pairs.

In practical situations, very often we need to warp image objects of arbitrary shapes. One of the main concerns is the warping of the boundary contours of the objects in a controllable way, such as the example shown in figure 1. The matching of corresponding pairs in existing methods may be very time consuming if a fine approximation is required. It is because they are not based on mapping contours and the computational cost is proportional to the number of feature pairs specified. In this paper, we introduce a new warping technique called *contour-based warping* that warps objects with arbitrary contours in a controllable way, and two warping methods that are based on this new warping technique.

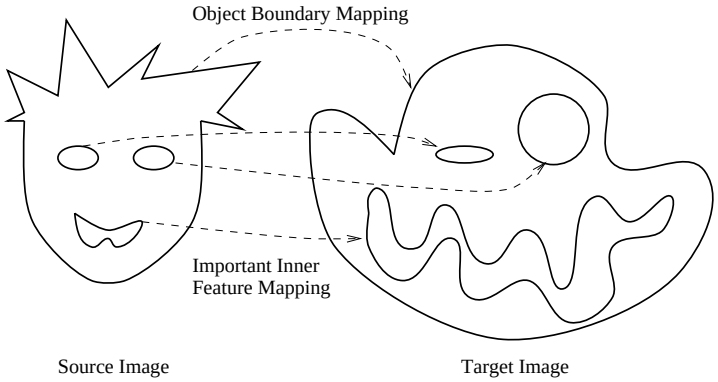

Figure 1: Warping of image objects with arbitrary contours.

The two warping methods introduced are the *peel-and-resample* method and the *wave propagation* method. The peel-and-resample method is fast and simple. It can warp an object with a single feature inside. However, it suffers from the problems of misalignment and inability of handling multiple inner-features, as will be discussed in section 3.4. The wave propagation method solves these two problems. It warps an image in a manner similar to wave propagated from the defined feature contours. Results show that the increase in the number of specified contour features distributed on the warping image can reduce the computational time. This indicates that, unlike other existing methods, the computational time of this method is not proportional to the number of features used. However, compared with the peel-and-resample method, a longer computational time is required when warping simple objects with a single inner-feature.

The rest of the paper is organized as follows. Section 2 describes the basic concept of contour-

based warping. Section 3 presents the peel-and-resample method while section 4 presents the wave propagation method. Finally, section 5 draws a conclusion of this paper and discusses possible future directions.

2 Principle Concept of Contour-Based Warping

To develop a warping technique which warps image objects with arbitrary shapes, we have proposed the idea of seeking the contour correspondence of the source and target images in our earlier paper [5]. Contour pairs are determined and those in the source are mapped onto those in the target, as shown in figure 2.

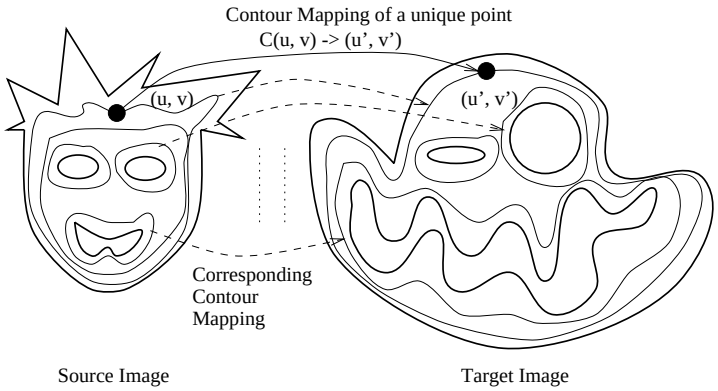

Figure 2: Idea of contour mapping for image warping.

Ideally, a mathematical model should be used to map each point from the source to the target. In continuous domain, given a set of contour pairs

$$\{(C_1, C_1'), (C_2, C_2'), ..., (C_n, C_n')\}$$

where contour C_i can be considered as a continuous parametric function that maps $[0, 1]$ to $\Re^2$. We define a continuous mapping function, C_Warp, which maps each point (u, v) in source domain to point (u', v') in target domain :

$$(u', v') = C\_Warp(u, v)$$

such that $(u', v') \in C_i' \Rightarrow (u, v) \in C_i, i \in [1, n]$

However, there is no easy way to mathematically define the correct contour correspondence of arbitrary planar objects as in figure 2. Here, we apply mathematical morphology in finding the contour correspondence. Mathematical morphology is a special branch of nonlinear image processing. One of its main applications is simplifying images and preserving the main shape of objects. It has been used in image preprocessing, such as shape simplification and noise filtering, and enhancing structures of image objects such as thinning and thickening. A morphological operation is given by the relation of the image object, I, with another structuring element set, S. The structuring element set is applied to each spatial point of the image object with the specified relation. Two basic morphological operators are used in this paper : *erosion* and *dilation*. Mathematically, erosion is a vector subtraction operation of the structuring element set to the image object while dilation is a vector addition.

$$erosion(I,S) = \{x|(x+s) \in I, \forall s \in S\} \quad (1)$$

$$dilation(I,S) = \{x|x = i+s, \forall i \in I, \forall s \in S\} \quad (2)$$

Theoretically, mathematical morphology can be applied to continuous domain. However, digital version is mostly handled in practical situation. A detailed introduction of mathematical morphology can be obtained from related materials [7][9][16].

Our contour-based warping is initially based on a *peel-and-resample* method. It is efficient but it suffers from the misalignment problem and the inability of handling multiple inner-features. A second method, called the *wave propagation* method, was then developed. This method overcomes the two limitations of the peel-and-resample method. However, it is slower than the peel-and-resample method when warping objects with a single inner-feature.

3 Peel-and-Resample method

The very first inspiration of this method was drawn from a skeleton-based warping method introduced by [18]. A planar image object with arbitrary shape is warped to another based on a skeletal thinning technique. The image is partitioned into layers, similar to peeling an object. A three pass resampling process is then performed to transform the layers firstly to a rectangular form in the original space, then to the rectangular form in the output space and finally to the output image. However, no consideration has been made on the warping effect inside the object and no control has been given on how to change the features inside the image object. Our peel-and-resample method solves this problem. In this method, the contours are determined/peeled by two morphological operators : *erosion* and *dilation*. The peeled contours are then resampled to a standard rectangular shape for mapping.

3.1 Erosion-Based Contour Determination

The erosion operator can be realised as a set operation which uses vector subtraction of elements, or pixels in image processing. This effect is equivalent to eroding an object layer by layer. The eroded layer can be treated as the corresponding contour away from the original boundary. To determine the corresponding contour pairs of the original and final objects, the peeled contours or layers of the original object (obtained by eroding function E_s) is transformed onto a rectangular grid (by rectangularization function R_s) and then resampled to the contours of the final image (by inverse of destination eroding and rectangularization functions $E_d^{-1}R_d^{-1}$). Figure 3 shows the process of warping an object by using the erosion operator.

Thus, each point p in the source is mapped to p' in the destination :

$$p' = Erode(p) = E_d^{-1}(R_d^{-1}(R_s(E_s(p)))) \tag{3}$$

When determining the contours between the boundary of an object and its inside feature, erosion provides no control of the warping effect inside the outer boundary. Under such situation, the dilation operator can be used to extract the corresponding contours.

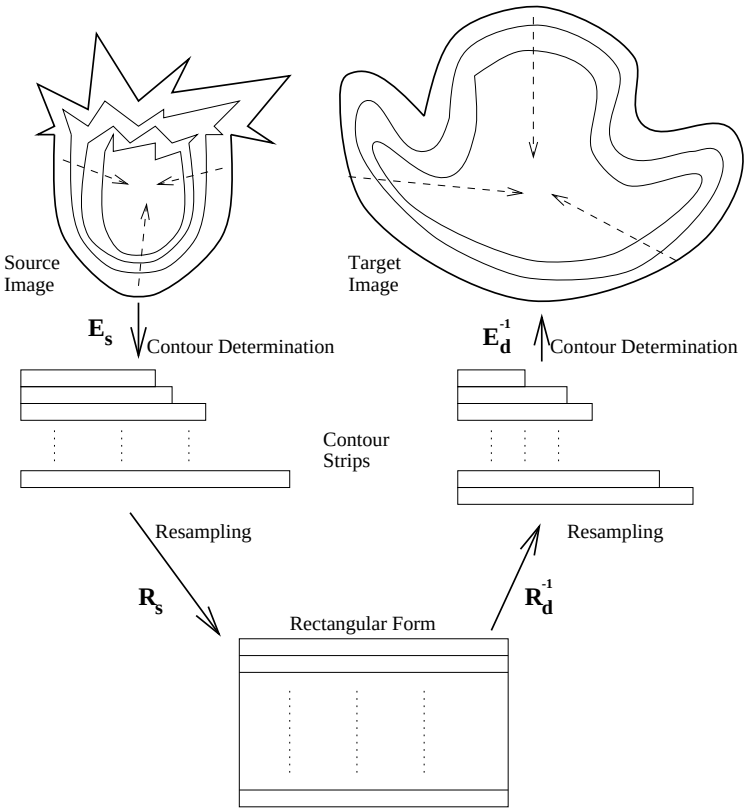

Figure 3: Principle of warping using the erosion operator.

3.2 Dilation-Based Contour Determination

Let us imagine that a stone with an arbitrary shape is thrown into the water. When the stone has just made contact with the water surface, water wave starts forming and propagating outwards. This process is similar to the dilation operation in mathematical morphology, which expands an object layer by layer in all directions.

Analogous to the water wave phenomenon, when an image object with an inner-feature is required to be warped in a controllable way, we treat the inside object as the stone being thrown. A dilation operator can be used to determine the "propagating water waves", and thus the contours between the main object boundary and the boundary of the inner-feature. The peeling of the object layers starts from the boundary of the inside feature and proceeds outwards as shown in figure 4.

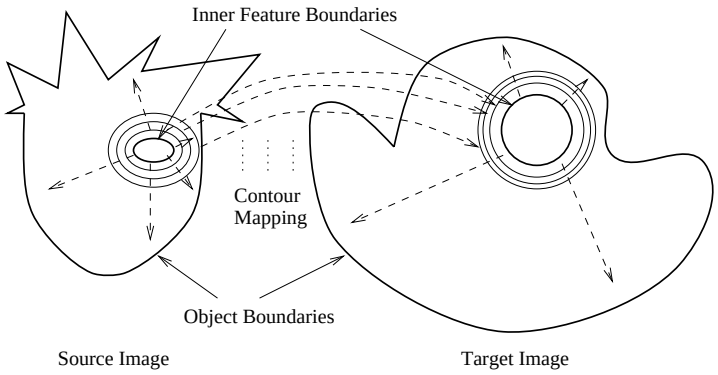

Figure 4: Contour determination using dilation.

Ideally, the contours have to be determined mathematically and correctly in order to have an accurate mapping of the corresponding contour pairs. However, erosion and dilation are pixel-based operations which process the image in pixel interval. Thus, the ideal contour which in fact may be fractional in pixel space cannot be obtained by these two primary morphological operators. In our dilation case, we connect the contour segments which have reached the boundary with the boundary contour as shown in figure 5. However, this causes the awkward warping effect where a large area of the boundary of the final image has the same pixel values.

To solve this problem, additional resampling of the rectangular grid is suggested here to get

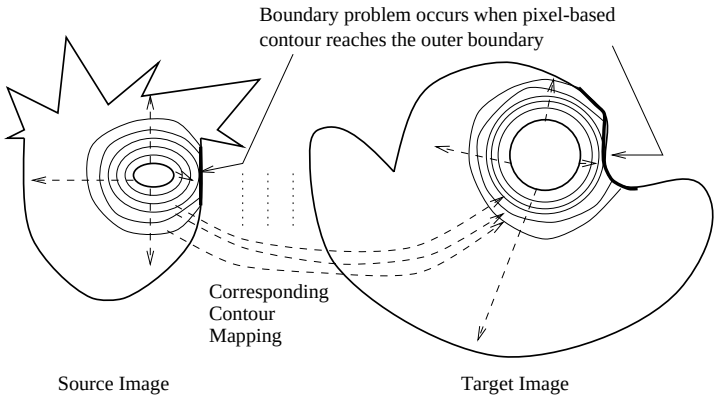

Figure 5: Boundary problem of dilation in determining contours.

rid of the duplicated boundary pixels so that a correct contour can be approximated as shown in figure 6. In the diagram, the black areas represent the overlapping regions of the contour strips. These areas are removed in the additional resampling operation. Similar to the Eroding function, each point p in the source is mapped to p' in the destination by

$$p' = Dilate(p) = D_d^{-1}(R_d^{-1}(B_d^{-1}(B_s(R_s(D_s(p)))))) \tag{4}$$

3.3 Warping Objects with a Single Inner-Feature

To warp an object with a single inner-feature, we separate the problem into two parts. In the first part, we treat the single inner-feature as a warping object without inner-feature. We use the erosion operator to determine the warped position of each point inside this inner-feature. In the second part, we handle the region between the inner-feature and the object boundary. Dilation operation is used and each point in this region is mapped according to the determined contour mapping.

Thus, given a set of non-overlapping feature contour pairs with two elements only,

$$\{(C_1, C_1'), (C_2, C_2')\}$$

where (C_1, C_1') is the object boundary contour pair and (C_2, C_2') is the boundary contour pair of

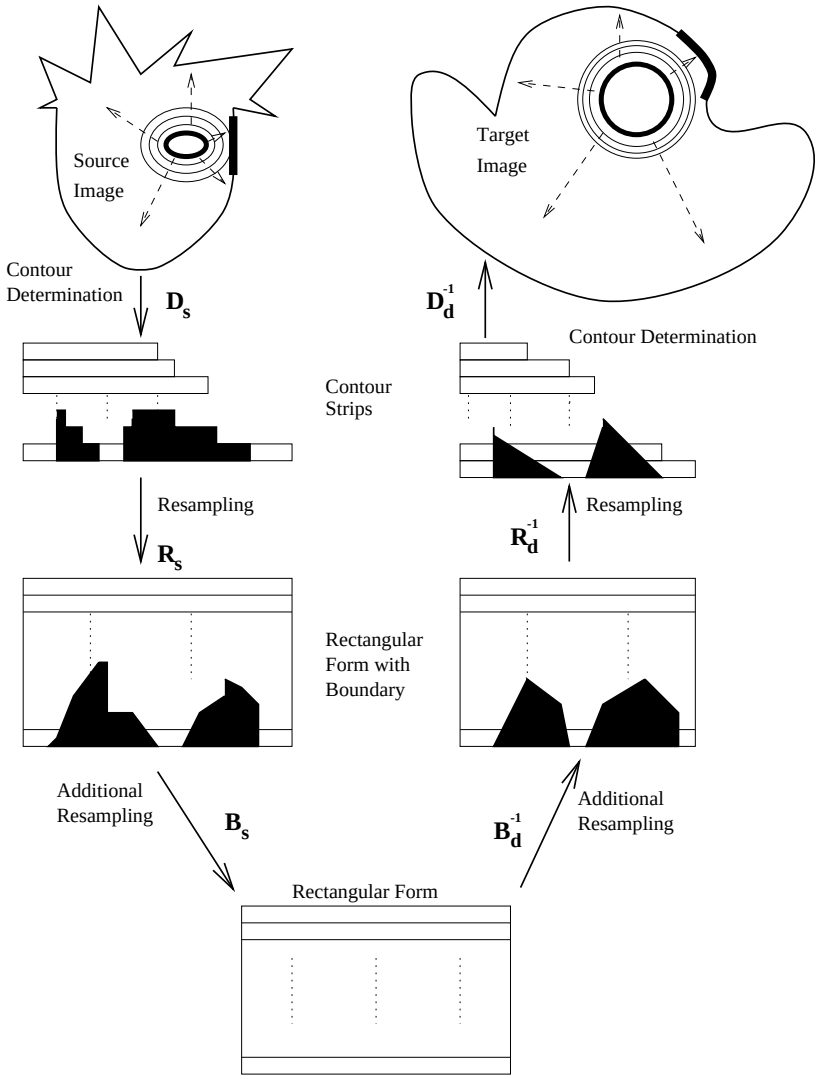

Figure 6: Handling the boundary problem of dilation.

the inner-feature, we solve the problem by using the Erode-Dilate E_D function below :

$$E\_D(u,v) = \begin{cases} Erode(u,v) & \text{if } (u,v) \text{ inside } C_2 \\ Dilate(u,v) & \text{otherwise} \end{cases} \tag{5}$$

3.4 Results and Discussions

Figure 7 demonstrates some results of this method. Image *a* shows a human head of resolution 201×263. Image *b* shows the dilated contours between the object boundary (the face silhouette) and an inner feature (the nose), while image *c* shows the input image overlaid with the determined contours. The contours inside the inner feature were determined by using the erosion operator and warped directly. The contours between the object boundary and the inner feature were determined by using the dilation operator. Image *d* shows target shapes of the face and the nose. Image *e* is the warped image from source *b* to target *d*. The resampled rectangular form $R_s(D_s(p))$, the boundary removed rectangular form $B_s(R_s(D_s(p)))$, and the mapped rectangular form $B_d^{-1}(B_s(R_s(D_s(p))))$ are shown in the top, middle and bottom diagrams of image *f* respectively. Note that the defined contours of the head and the nose in the destination mask are irregular, and the image is warped to a funny shape. We tested the program on a SUN SPARC 10 system and the processing time required to produce the warped image was about 2.5 seconds. The computational time is only proportional to the size of the specified region, thus the region inside the face silhouette in this example of the image, of the image to be warped.

However, two basic problems were found and needed to be solved - the misalignment problem and the inability of handling multiple inner-features. The *misalignment problem* is that some pixels may not be able to retain the neighborhood relationship with their adjacent pixels after the warping process. Images *h* and *i* in figure 7 show an example of this case. The warped image *h* is generated by mapping the source contours in image *b* to those in image *g*. We can see that the eye region of the warped face is misaligned. Image *i* shows the magnification of the warped eye region. It clearly illustrates the misalignment problem. For a continuous and smooth mapping, the spatial adjacency of pixels must be maintained.

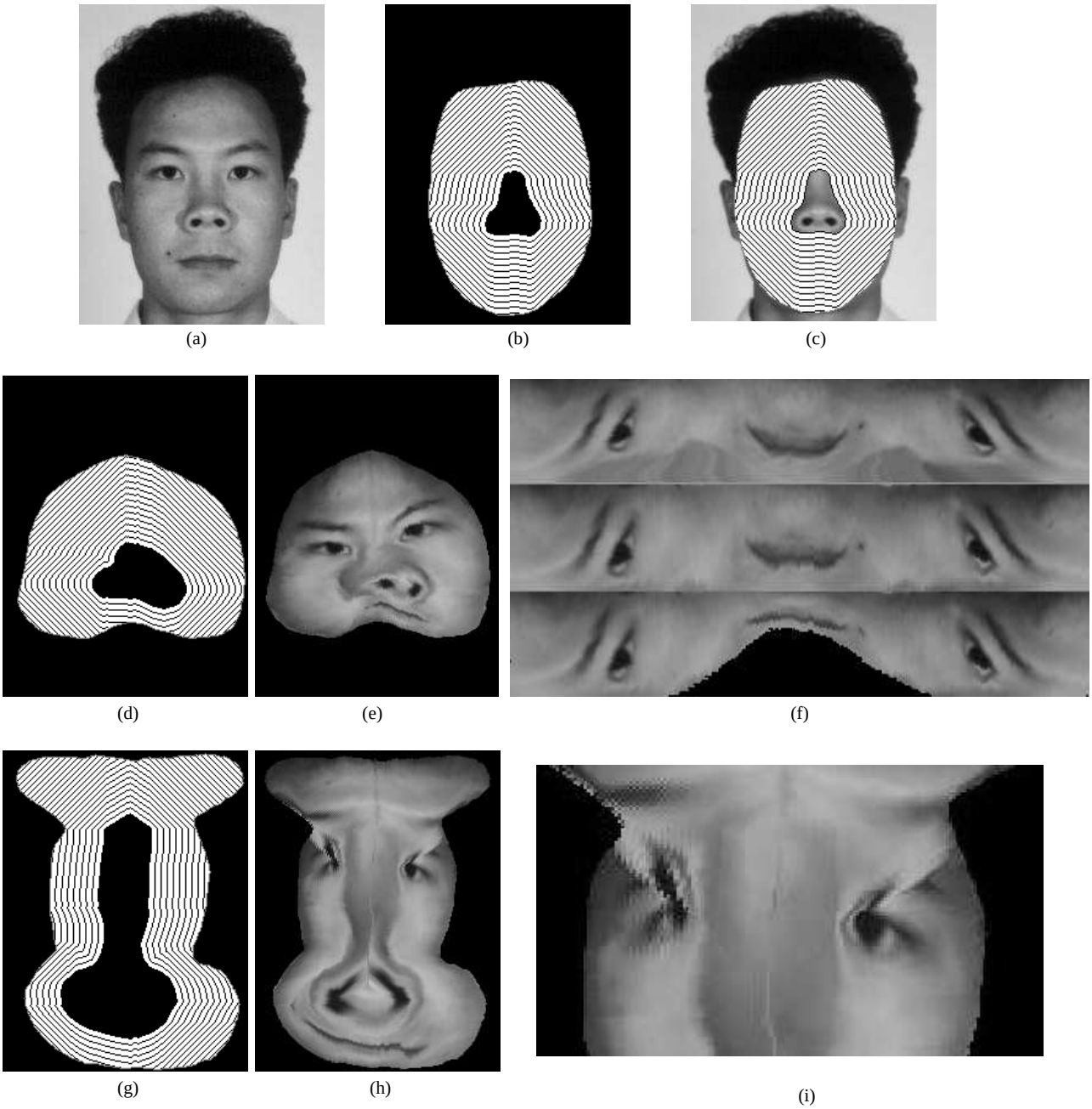

Figure 7: Results of the peel-and-resample method.

The second problem is that the peel-and-resample method can only handle objects with a single feature inside. In the case of multiple inner features, the whole warping process needs to be solved by a weighted sum approach of partitioned sub-problems. Each sub-problem consists of the object boundary and one of the inner features only. It is simply a single inner-feature problem discussed in section 3.3. However, this cannot guarantee an appropriate warping and the desired warping effect may not be obtained. Wave propagation method is introduced to solve these problems. It warps an image in a manner similar to wave propagation.

4 Wave Propagation Method

In wave propagation method, the misalignment problem of the peel-and-resample method is overcome by introducing linking force to maintain the geometrical relationship of neighboring pixels. This effectively forms a linking grid to the image. As such, image warping can be realized as deforming a linking grid by wave propagation based on specified feature contours.

4.1 Equilibrium of the Linking Grid

In order to maintain the neighborhood relationship, each spatial point in the image domain is connected to adjacent neighboring points by linking forces. Here, we only consider preserving the relationship of 4-connected neighborhood. As shown in figure 8, the neighborhood relationship of the center pixel with the 4 adjacent pixels (drawn in black dot) is retained by the linking force. Other non-neighbors are kept away from the linking force region.

At equilibrium state of the linking grid, any point p having the set of neighboring pixels N_p :

$$\sum_{q \in N_p} F_l(p,q) + F_a(p) = 0 \tag{6}$$

where $F_l(p,q)$ is the linking force between points p and q. $F_a(p)$ is an additional force used to characterize the warping effect. For example, we may consider $F_a(p)$ as a friction force. When it is equal to zero, the linking grid will be formed in a way that all pixel will tend to be evenly

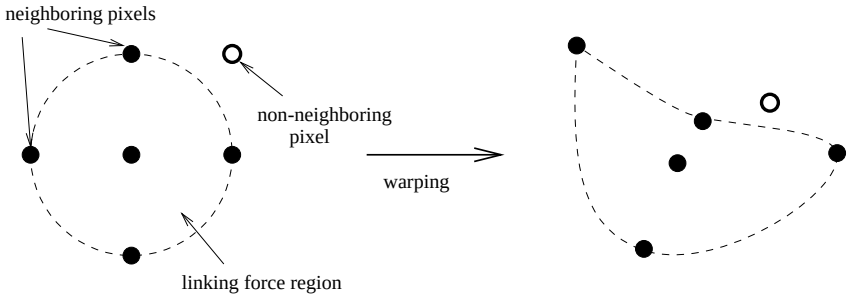

Figure 8: Maintaining the neighborhood relationship by linking forces.

distributed. When it is a reaction force with factor proportional to the distance of the pixel p from the defined contour, the warping will tend to be localized. Because solving the equilibrium problem mathematically is impractical, we use an iterative approach in the implementation of the method instead.

4.2 Wave Propagation

Given a set of n feature contour pairs :

$$C = ((C_1, C_1'), (C_2, C_2'), ..., (C_n, C_n'))$$

where C_i and C_i', $i \in [1, n]$, are the source and the corresponding target contours. When warping starts from anchoring each given source contour C_i to the position of its corresponding destination contour C_i', its neighbors start moving accordingly. The linking force will force the adjacent neighbors to shift to the new positions such that the linking force between them can be minimized to zero. Similar to the concept of wave propagation, the "moving wave" will propagate from the given source contours to their neighbors layer by layer. Thus image warping becomes a process of deforming the linking grid.

As mentioned earlier, because solving the equilibrium problem mathematically is impractical, we use an iterative approach in the implementation of the technique. In each iteration cycle, each pixel which is close to the feature contours is firstly moved to a new position so that the summation of all its linking forces is close to zero. Then the process will propagate to pixels further away from

the feature contours. The iteration cycle continues until an equilibrium state is reached. The process of deforming a checkerboard image through wave propagation is illustrated in figure 9. The original rectangular feature contours in black color are mapped to the destination feature contours having arbitrary shape in white color as shown in the original checkerboard image *a*. The waves start propagating from the "anchored" feature contours outwards and their immediate neighbors are then displaced according to equation 6. These neighbors further propagate the wave to the rest of the image. Images *b* and *c* show the warped images after 10 and 30 iterations respectively of wave propagation. The final warped checkerboard at its equilibrium state after 93 iterations is shown in image *d*.

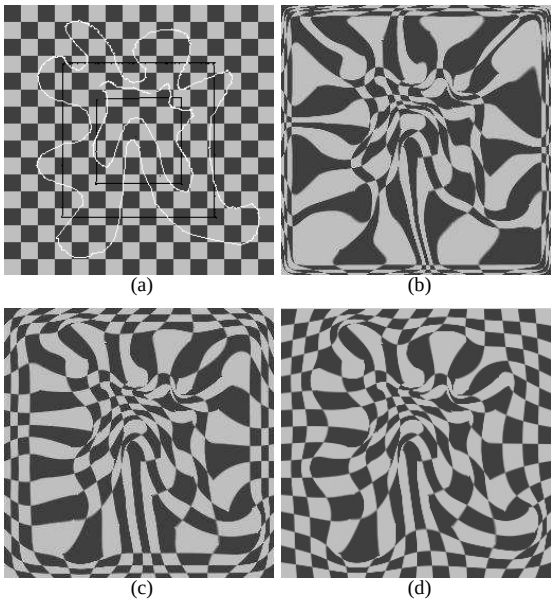

Figure 9: Warping of a checkerboard image using wave propagation.

In addition to solving the misalignment problem, this method also solves the problem of handling multiple inner-features in the peel-and-resample method naturally. There is no limitation on how many inner-features can be specified. The new warping process is equivalent to anchoring the feature contour in a linking grid, and adjusting the locations of other grid nodes until a equilibrium state is obtained. The following shows the pseudo code of the method. Given the input image "InputImage", the specified contour features of the source domain "source-contours", and the specified contour features of the target domain "target-contours",

*Determine-contours(*InputImage,determined-contours*)*

*Anchor(*source-contours *to* target-contours*)*
While (if not-equilibrium)
from source-contours *outwards*
for each pixel p in determined-contours
if $\sum_{q \in N_p} F_l(p,q) + F_a(p) \neq 0$
move p so-that $\sum_{q \in N_p} F_l(p,q) + F_a(p) = 0$
EndWhile

The function *Determine-contours()* determines other corresponding contours, "determined-contours", for wave propagation in the image space based on "source-contours" and "target-contours".

4.3 Results and Discussion

We have implemented this wave propagation method and some results have been obtained. We use the simple vector $\vec{pq}$ as the directional linking force $F_l(p,q)$, which has the magnitude directly proportional to the distance between two neighboring nodes p and q.

$$F_l(p,q) = \vec{pq}$$

We also treat the additional force, $F_a(p)$, as a special friction force based on a critical force F_c:

$$F_a(p) = \begin{cases} 0 & \text{if } |\sum F_l(p,q)| > |F_c| \\ -\sum F_l(p,q) & \text{otherwise} \end{cases}$$

When the magnitude of the total linking force $\sum F_l(p,q)$ is larger than that of the critical friction force F_c, there will be no reaction force against the pixel node and $F_a(p)$ is equal to zero. The net force will force the pixel node to move to a new position such that the new net force is close to zero. However, when the total linking force is equal to or smaller than the critical force, the friction force will react as an opposite force totally against the total linking force and keep the pixel node in the same position.

4.3.1 Maintaining Alignment

Figure 10 shows the warped image based on contour features specifying the facial silhouette and nose. The specified contours are those used to produce image *i* of figure 7 in the peel-and-resample method. The human contours are shown in image 7*b* and the ape contours are shown in image 7*g*. In figure 10, the left image shows the mapping vectors from the source position to the target position. The warped human face is shown on the right. It clearly illustrates that the image is smoothly warped to the desired shape and the misalignment has been overcome. However, it took 109 iterations before reaching the equilibrium state. The overall time required to produce the image is about 31 seconds. Compared with the peel-and-resample method, this method requires a longer computational time for warping an image object with a single inner-feature.

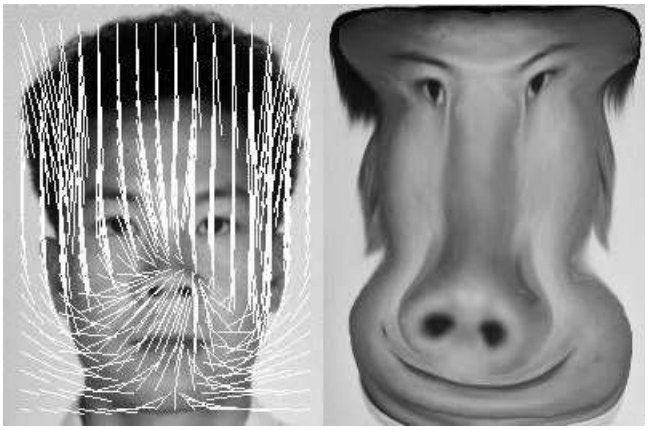

Figure 10: Result of maintaining alignment.

4.3.2 Warping Effect of Multiple Inner Features

Figure 11 shows the effect of warping multiple inner features by using the wave propagation method. A human face is warped to the shape of an ape in the left column, while the ape is warped to the shape of the human in the right. Images *a* and *b* show the original faces and their corresponding facial features. These feature contours are specified in terms of arbitrary shapes which fit the actual boundaries of the facial features. Images *c* and *d* indicate the determined contours overlaid

on the images. Images e and f show the intermediate deforming frames after 10 iterations of wave propagation. Note that the images have basically been warped appropriately, especially in the regions nearby the defined contours. Images g and h show the vectors of mapping from source to the target, while images i and j are the final warped images after 109 and 97 iterations respectively.

4.3.3 Effect of Specifying Additional Features

Figure 12 shows similar warping operations of figure 11. However, there are two extra feature contours specified beside the left and right cheeks as shown in image a. The specified feature contours of the source domain are shown in black color and those of the target domain are shown in white. Image b is obtained after 10 iterations. This intermediate warped image is very close to the final one as shown on the right. The final warped image c requires only 70 iterations of wave propagation to reach the equilibrium state. Compared with figure 11i which needs 109 iterations, this requires only 64% of the original computational cost to obtain a similar warping effect. Hence, unlike other existing warping techniques, the computational time of this method is not proportional to the number of features specified. On the contrary, it can be reduced with additional features distributed on the image as demonstrated in this example. It is only affected by the size of the image and the maximum displacement from the source contour to the target one, which may alter the number of wave iterations required to reach the equilibrium state. All examples shown here were produced on a SUN SPARC 10 system. It took 31 and 21 seconds to generate images 11i and 12c respectively. However, this method requires longer computational time compared with the peel-and-resample method when warping simple images with a single inner-feature.

4.3.4 Effect of Overlapping Contours

During our investigation of the problem, we have found that unpredictable warping effect is obtained when some defined contours overlap each other. It leads to an irreversible "folding" effect, which is also a common problem of other image warping methods. Figure 13 shows two examples of this overlapping problem. Image a shows the newly defined target contours (in white curves) of the ape

and image b is the warped image. The source contours of the human are the same as those shown in figure 11a. Note that the specified contours of the ape's mouth and nose are overlapped and this causes the strange warping effect around the region. Another example is shown in images c and d. Image c shows an original checkerboard with two rectangular source contours in black and two overlapping target contours in white, while image d shows the warped checkerboard with strange folding effect in the overlapping regions near the six intersection points.

4.3.5 Method Applied in Morphing

Figure 14 shows the synthesized images of applying the new warping method to produce morphing effect using the human image in figure 11a and the ape in figure 11b. The same sets of feature contours are specified. This figure is an example of morphing effect using the common "warp and cross-dissolve" approach. The left column of images in the figure is the result of pixel interpolation between a set of warped ape images and the images in the right column of the figure. The images on the left column of figure 14 are the intermediate frames of the morphing process and produces the effect of transforming a human head to an ape face smoothly. The warped images of the human for the morphing process are shown on the right. Note that the human face is warped to the desired shapes. An additional morphing example by using the new method is shown in figure 15, which transforms a mouse to a cat.

5 Conclusion and Future Directions

Contour-based warping has been presented. It allows image features to be defined naturally in terms of contours, instead of point, vector or patch based features in conventional methods. Two methods based on mapping contours, the peel-and-resample and the wave propagation methods, are introduced in this paper.

The peel-and-resample method is a fast and simple technique, which can warp an object with a single feature inside. However, it suffers from the problems of misalignment and inability of

handling multiple inner-features. Wave propagation method warps an image in a manner similar to wave propagation from the defined feature contours. The method solves the misalignment problem of the peel-and-resample method by introducing linking force, and can handle multiple inner-features naturally. Linking force is applied to neighboring pixels for maintaining the neighborhood relationship. Results of warping objects with arbitrary features show that the method warps the image objects to the desired shapes. Furthermore, additional investigations show that the increase in the number of specified contour features distributed on the warping image can reduce the computational time. This indicates that, unlike other existing methods, the computational time of this method is not proportional to the number of features used. However, compared with the peel-and-resample method, a longer computational time is required when warping simple objects with a single inner-feature. Some morphing results using this method are also given.

In order to reduce the computational time required in the wave propagation method, we are planning to investigate a multi-resolution approach of the method and the application of a more sophisticated iterative methods. The image may be subsampled to smaller images with different resolutions of the original. Together with subsampled feature contours, the subsampled image with the lowest resolution will firstly be warped by the technique. The warped linking grid will be used to guide the warping process applied to the higher resolution image and so on until the original one. This method can reduce the overall computational time. It can also provide a real time interaction where we can trade off between the quality of the warped image and the speed of the interaction. On the other hand, the iterative algorithm used in our implementation presented in section 4.2 is basically a Gauss-Seidel iteration method. Some other preconditioned iterative methods, such as Conjugate Gradients, GMRES and QMR, generally can converge much faster [15]. They can be used in future enhancements of the technique.

The new method can also be used to assist further development of a semi-automatic motion morphing system and a model-based image coding system when accompanied with robust feature extractors, as proposed in our earlier paper [5]. The proposed work presented in [6] is also a good reference for developing this system, by integrating automatic matching method and active contour

model with our new warping technique. In addition, the extension of this 2D method to 3D warping and morphing of 3D volumetric data is also being investigated.

6 Acknowledgement

We would like to thank the anonymous reviewers for their useful and constructive comments. The authors also gratefully acknowledge the help and advice of the people in the graphics research team of the Hong Kong Polytechnic University.

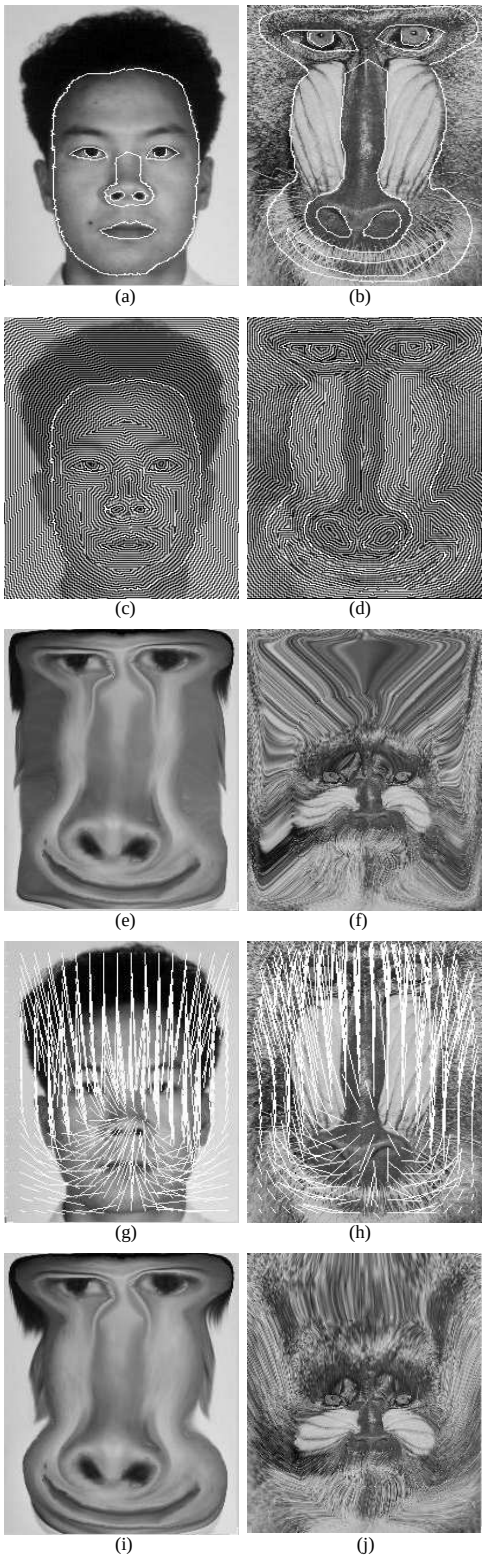

Figure 11: Warping with multiple inner features.

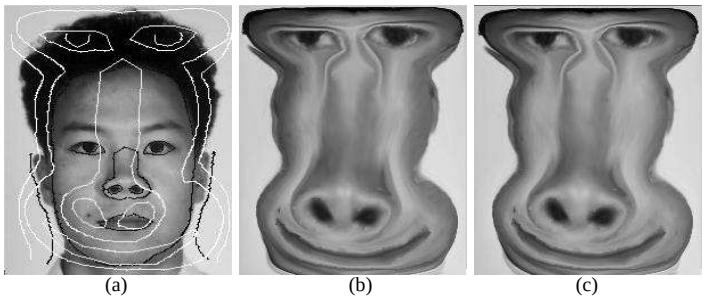

Figure 12: Example of reducing computational time by adding extra feature contours.

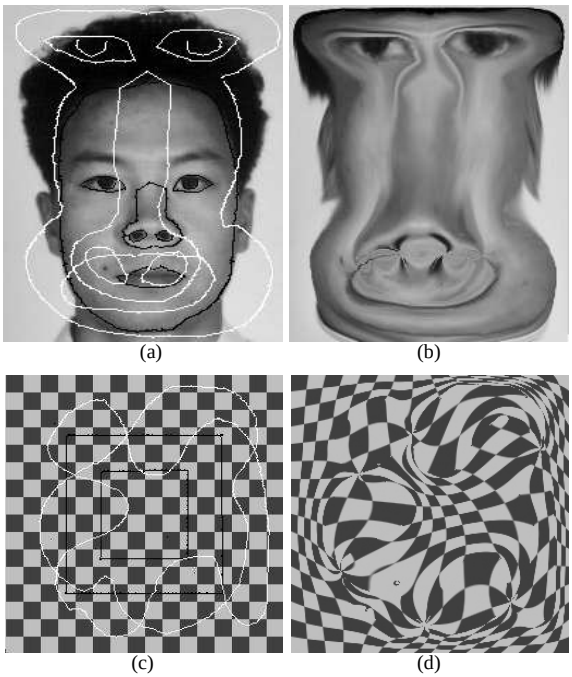

Figure 13: Example of the overlapping effect.

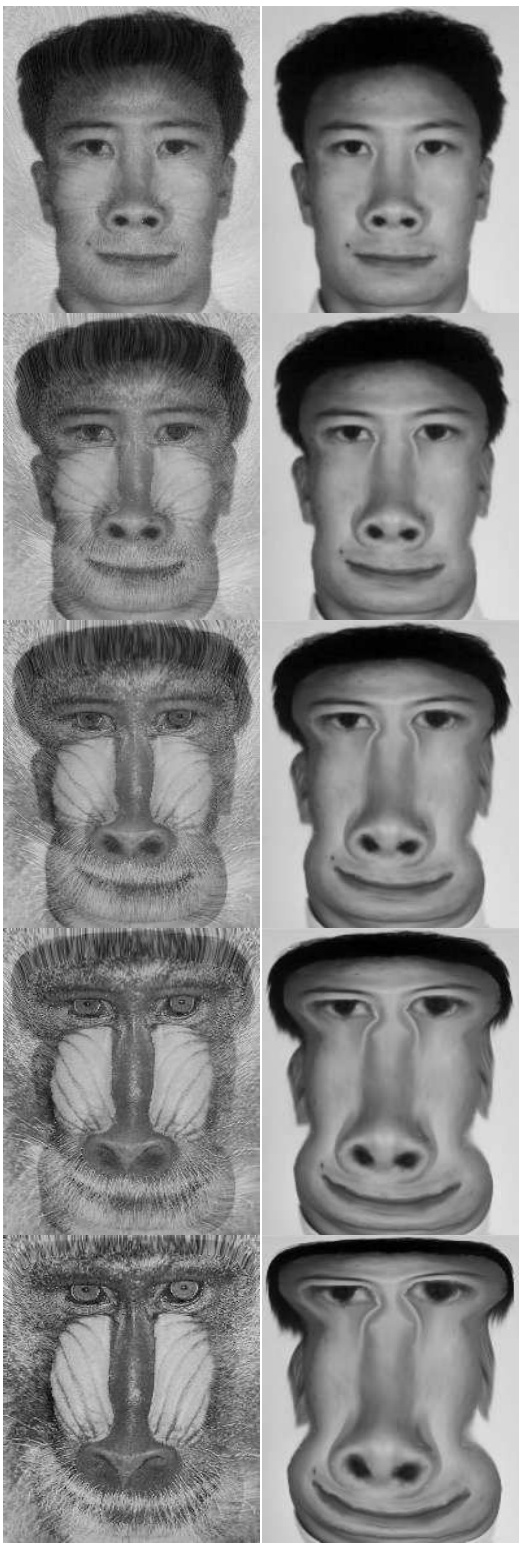

Figure 14: Morphing from human to ape.

Figure 15: Morphing from mouse to cat.

References

[1] N. Arad, N. Dyn, D. Reisfeld, and Y. Yeshurun, *Image warping by radial basis functions: Application to facial expressions*, CVGIP : Graphical Models and Image Processing, 56 (1994), pp. 161–172.

[2] I. Barrodale, D. Skea, M. Berkley, R. Kuwahara, and R. Poeckert, *Warping digital images using thin plate splines*, Pattern Recognition, 26 (1993), pp. 375–376.

[3] T. Beier and S. Neely, *Feature-based image metamorphosis*, Computer Graphics, 26 (1992), pp. 35–42.

[4] F.L. Bookstein, *Principal warps: Thin-plate splines and the decomposition of deformations*, IEEE Transactions of Pattern Analysis and Machine Intelligence, 11 (1989), pp. 567–585.

[5] K.H. Chan and R.W.H. Lau, *Contour-based image warping*, Electronic Imaging and Multimedia Systems, Proc. SPIE 2898, (1996), pp. 306–316.

[6] M. Covell, *Autocorrespondence: Feature-based match estimation and image metamorphosis*, Proc. IEEE International Conference on Systems, Man and Cybernetics, (1995), pp. 2736–2741.

[7] E.R. Dougherty, *An Introduction to Morphological Image Processing*, SPIE Optical Engineering Press, Washington, 1992.

[8] C. Frederick and E.L. Schwartz, *Conformal image warping*, IEEE Computer Graphics and Applications, (1990), pp. 54–61.

[9] C.R. Giardina and E.R. Dougherty, *Morphological Methods in Image and Signal Processing*, Prentice-Hall, Inc., USA, 1988.

[10] P. Heckbert, *Fundamentals of texture mapping and image warping*, Master Thesis, University of California, Berkeley, (1989).

[11] P. Landau and E. Schwartz, *Subset warping : Rubber sheeting with cuts*, CVGIP : Graphical Models and Image Processing, 56 (1994), pp. 247–266.

[12] S. Lee, K. Chwa, S.Y. Shin, and G. Wolberg, *Image metamorphosis using snakes and free-form deformations*, Computer Graphics, (1995), pp. 439–448.

[13] S. Lee, G. Wolberg, K. Chwa, and S.Y. Shin, *Image metamorphosis with scattered feature constraints*, IEEE Transactions on Visualization and Computer Graphics, 2 (1996), pp. 337–354.

[14] D. Ruprecht and H. Muller, *Image warping with scattered data interpolation*, IEEE Computer Graphics and Applications, (1995), pp. 37–43.

[15] Y. Saad, *Iterative Methods for Sparse Linear Systems*, PWS Pub. Co., Boston, 1996.

[16] J. Serra, *Image Analysis and Mathematical Morphology*, Academic Press, London, 1982.

[17] A.R. Smith, *Planar 2-pass texture mapping and warping*, Computer Graphics, 25 (1987), pp. 263–272.

[18] G. Wolberg, *Skeleton-based image warping*, The Visual Computer, 5 (1989), pp. 95–108.

[19] G. Wolberg, *Digital Image Warping*, IEEE Computer Society Press, Washington, 1990.